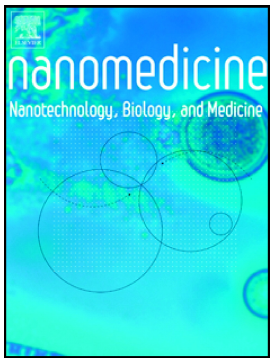

Hyaluronic acid-based nanogels improve in vivo compatibility of the anti-biofilm peptide DJK-5

Sylvia N. Kłodzińska, Daniel Pletzer, Negin Rahanjam, Thomas Rades, Robert E.W. Hancock, Hanne M. Nielsen

PII: S1549-9634(19)30106-6
DOI: https://doi.org/10.1016/j.nano.2019.102022
Article Number: 102022
Reference: NANO 102022

To appear in: *Nanomedicine: Nanotechnology, Biology, and Medicine*

Revised date: 18 May 2019

Please cite this article as: S.N. Kłodzińska, D. Pletzer, N. Rahanjam, et al., Hyaluronic acid-based nanogels improve in vivo compatibility of the anti-biofilm peptide DJK-5, Nanomedicine: Nanotechnology, Biology, and Medicine, https://doi.org/10.1016/j.nano.2019.102022

Hyaluronic acid-based nanogels improve *in vivo* compatibility of the anti-biofilm peptide DJK-5

Sylvia N. Kłodzińska PhD[1], Daniel Pletzer PhD[2], Negin Rahanjam MSc[2], Thomas Rades Professor[1], Robert E. W. Hancock Professor[2] and Hanne M. Nielsen Professor[1]*

[1] *Department of Pharmacy, Faculty of Health and Medical Sciences, University of Copenhagen, Universitetsparken 2, DK-2100 Copenhagen, Denmark*

[2] *Centre for Microbial Diseases and Immunity Research, Department of Microbiology and Immunology, University of British Columbia, Vancouver, Canada*

*****Correspondence: hanne.morck@sund.ku.dk; Tel.: +45-3533-6346

Funding sources

The authors acknowledge financial support from the University of Copenhagen 2016 Programme of Excellence Research Centre for Control of Antibiotic Resistance (UC-CARE) (SNK). DP received a Cystic Fibrosis Postdoctoral fellowship (Canada) and REWH is supported by Canadian Institutes from Health Research grant FDN-154287 and holds a Canada Research Chair and UBC Killam Professorship. Equipment funding was achieved from the Danish Agency for Science, Technology and Innovation (DanCARD, grant no. 06-097075).

Conflict of interest

The DJK-5 peptide described here has been filed for patent protection by REWH and co-inventors, assigned to REWH's employer, the University of British Columbia, and licenced to ABT Innovations Inc., Victoria, Canada, in which the University of British Columbia and REWH own shares.

Word count for abstract: 149
Complete manuscript word count: 4,981
Number of references: 59
Number of figures: 6
Number of tables: 1

Abstract

Anti-biofilm peptides are a subset of antimicrobial peptides and represent promising broad-spectrum agents for the treatment of bacterial biofilms, though some display host toxicity *in vivo*. Here we evaluated nanogels composed of modified hyaluronic acid for the encapsulation of the anti-biofilm peptide DJK-5 *in vivo*. Nanogels of 174 to 194 nm encapsulating 33 – 60% of peptide were created. Efficacy and toxicity of the nanogels were tested *in vivo* employing a murine abscess model of a *Pseudomonas aeruginosa* LESB58 high bacterial density infection. The dose of DJK-5 that could be administered intravenously to mice without inducing toxicity was more than doubled after encapsulation in nanogels. Upon subcutaneous administration, the toxicity of the DJK-5 in nanogels was decreased four-fold compared to non-formulated peptide, without compromising the anti-abscess effect of DJK-5. These findings support the use of nanogels to increase the safety of antimicrobial and anti-biofilm peptides after intravenous and subcutaneous administration.

Keywords: biofilm; *Pseudomonas aeruginosa*; cationic peptide; nanogel; drug delivery

Background

Chronic bacterial infections of the skin and soft tissues constitute a common problem [1], accounting for 6.8 million hospital consultations in emergency departments in the United States annually [2]. Although a major proportion of these infections are caused by *Staphylococcus aureus*, approximately one-fifth of the infections are caused by Gram-negative bacteria [3]. A Gram-negative pathogen that is often responsible for such infections is *Pseudomonas aeruginosa* [4], an opportunistic bacterium that also shows rapid development of acquired resistance [5]. The global threat of antimicrobial resistance emphasizes the need for novel treatment strategies, and anti-biofilm peptides, a distinct subset of antimicrobial peptides (AMPs), are a promising approach for combating multi-resistant biofilm infections [6,7]. Anti-biofilm peptides are short, cationic and amphipathic and can show strong broad spectrum antibiofilm activity [8,9]. However, AMPs are often susceptible to degradation by bacterial and host proteases present at the site of the infection [10], and some may show cytotoxicity and/or hemolytic properties towards eukaryotic cells [11,12]. Recently, a series of short protease-resistant D-enantiomeric peptides with broad-spectrum antibiofilm activity were designed [10]. One of the most potent antibiofilm peptides was DJK-5, which reduced sizes of abscess lesion caused by ESKAPE pathogens *in vivo*, as well as modestly reduced the number of colony forming units (CFU) at the infection site [13–15]. The peptide DJK-5 acts by binding to and triggering the degradation of the stress- related second messenger nucleotides guanosine penta- and tetraphosphate – two unusual nucleotides which play an important role in biofilm development in many bacterial species [10]. In order for DJK-5 to exert its activity it must be translocated across the cell membrane, a process for which the peptide's secondary structure is very important [16]. This peptide also decreased the size and the bacterial load of the subcutaneous abscesses *in vivo* at 1.25 – 1.5 mg/mL [13,14], therefore toxicity of DJK-5 above these

concentrations may not necessarily negate its future use. However, the therapeutic index can be increased by improving the compatibility of this peptide.

High cytotoxicity associated with cationic peptide exposure can be decreased by the use of nanogel drug delivery systems [17,18]. Nanogels are nano-sized cross-linked polymeric networks which may be used to encapsulate a variety of bioactive compounds, particularly peptides and proteins [19]. Nanogels may comprise a promising drug delivery system due to their excellent drug loading capacity [17], high structural stability [20], biocompatibility, and favourable responses to a wide variety of environmental stimuli, such as ionic strength [18], pH [20], and temperature [19,21].
In this study, the negatively charged polymer hyaluronic acid (HA) with a molecular weight of 50 kDa was investigated. HA is considered to be an excellent starting material for design of delivery systems as a result of its biocompatibility and ease of chemical functionalization [22]. Due to its lack of inherent amphiphilicity, HA cannot spontaneously assemble into stable, segregated nanogel structures in aqueous media. To render HA amphipathic, hydrophobic groups, such as octenyl succinic anhydride (OSA), are covalently grafted onto the polymer backbone [23]. The resulting functional polymer octenyl-succinic anhydride-modified hyaluronic acid (OSA-HA) has shown to spontaneously self-assemble into multiphasic submicron physically cross-linked nanogel particles and encapsulate a model hydrophobic compound [24]. Alkenyl-/aryl-succinic anhydrides (including OSA) have also been used to modify high molecular weight HA and have shown improved emulsifying properties compared to HA giving further stabilization in addition to the effect of the viscosity increase in the aqueous phase caused by polymer addition [25]. Initial studies on OSA-HA nanogels encapsulating a peptidomimetic have shown that this carrier system can also be used for encapsulation of AMPs and their derivatives [26]. The OSA-HA nanogels encapsulating the peptidomimetic LBP-3 decreased LBP-3 cytotoxicity compared to equimolar amounts of free peptidomimetic in solution, whereas the antimicrobial activity of LBP-3 remained unchanged or

was improved with the carrier system depending on the formulation conditions. However, the peptidomimetic release from the nanogels and the performance *in vivo* was not assessed.
Here, we assessed the physicochemical properties of nanogels composed of OSA-modified low molecular weight HA encapsulating the synthetic peptide DJK-5 to expand the therapeutic index for the application of this peptide. The toxicity of DJK-5 after encapsulation in nanogels was assessed *in vivo* after both subcutaneous and intravenous administration, whereas efficacy was evaluated *in vivo* using a murine abscess model [13,27] induced by a subcutaneous injection of *P. aeruginosa*.

Methods

Materials

Hyaluronic acid (HyaCare, 50 kDa) was purchased from Evonik Nutrition & Care (Essen, Germany). Octenyl succinic anhydride (OSA), as well as standard salts and buffers were obtained from Sigma-Aldrich (St. Louis, MO, USA). DJK-5 (vqwrairvrvir-NH_2; all D-amino acids) was synthesized and purified to >95% by CPC Scientific (Sunnyvale, CA, USA) or Synpeptide (Shanghai, China) and stored lyophilized until use. Analytical grade solvents for HPLC analysis were purchased from Merck (Darmstadt, Germany). Ultrapure water for synthesis of polymer, sample preparation and analysis was obtained from a PURELAB® flex 4 (ELGA LabWater, High Wycombe, UK).

Octenyl succinic anhydride-modified hyaluronic acid (OSA-HA) synthesis and characterization

OSA-HA (50 kDa, 24% degree of substitution) was prepared as described previously [22]. Briefly, 1.25 g HA was dissolved in 50 mL of ultrapure water, after which $NaHCO_3$ was added to yield a 2 M carbonate solution. The pH was then adjusted to pH 8.5 with NaOH, and OSA was added to the

HA solution dropwise to reach a 50:1 molar ratio of OSA:HA. This solution was left to react overnight at room temperature. Afterwards, the product was dialysed at 4 °C against ultrapure water and freeze-dried. The degree of substitution for OSA-HA was determined by ^{1}H NMR.

Nanogel preparation

Nanogels were produced at room temperature immediately prior to use. Both DJK-5 and OSA-HA were dissolved in ultrapure water. Briefly, a DJK-5 solution (10× final peptide concentration, i.e., 20-75 mg/mL) was added to a OSA-HA solution (6.66 – 25 mg/mL) resulting in a 0.3:1 (w/w) mixture ratio of DJK-5:polymer. The peptide and polymer solutions were vortexed briefly to form nanogels and used 1-2 h after preparation.

Nanogel size and surface charge

The average nanogel size and polydispersity index (PDI) were based on particle size distributions obtained by dynamic light scattering and the surface charge of the nanogels was estimated by the zeta potential (ZP). The size, PDI and ZP measurements were performed at 25°C using a Zetasizer Nano ZS (Malvern Instruments, Worcestershire, UK) equipped with a 633 nm laser and 173° detection optics. Malvern DTS v.6.20 software was used for data acquisition and analysis. Size, PDI and surface charge were determined in triplicate for three independent sample batch replicates.

Nanogel visualization

The nanogels were stained using uranyl acetate negative stain and visualized using transmission electron microscopy (TEM). A carbon-coated grid was glow discharged, after which 3 µL of nanogel dispersion was deposited on the surface and air dried for 1 min. After drying, 3 µL of 0.5%

w/v uranyl acetate solution were added for 2 min after which the grid was rinsed once and blotted with filter paper. Afterwards, samples were visualized using a CM100 (a) TWIN microscope (Philips/FEI, Hillsboro, OR, USA).

DJK-5 encapsulation and release

The encapsulation efficiency (EE) of DJK-5 was determined by measuring the amount of residual peptide in the aqueous bulk phase after nanogel production. The aqueous bulk phase was obtained after ultracentrifugation of nanogels at 500,000 × *g* for 30 min at 22 °C. Calculation was based on the theoretical drug loading (Eq. 1).

$$EE = \frac{Measured\ drug\ loading}{Theoretical\ drug\ loading} \times 100\% \quad (1)$$

Quantification of DJK-5

Quantification of DJK-5 concentrations was performed by using reverse phase high performance liqid chromatography on a Shimadzu Prominence system (Kyoto, Japan) using a Kinetex XB-C18 column (50 × 2.1 mm, 2.6 µm, Phenomenex, Torrance, CA, USA) measuring the absorbance at 218 nm. The mobile phase consisted of eluent A [95:5% (v/v) acetonitrile:water] and eluent B [5:95% (v/v) acetonitrile:water], which both contained 0.1% (v/v) TFA. Samples were run with a gradient of 0 → 50% eluent B over 5 min at 0.8 mL/min at 40 °C. The limit of detection and limit of quantification was 1.9 µg/mL and 6.5 µg/mL, respectively.

Structure of DJK-5 in nanogels

The secondary structure of non-formulated and formulated DJK-5 was investigated using circular dichroism (CD). Spectra were recorded using an Chirascan CD spectrometer (Applied

Photophysics, Leatherhead, Surrey, UK) with a 1 mm path length quartz cuvette. Both nanogel and non-formulated DJK-5 spectra were obtained at a peptide concentration of 0.125 mg/mL. The spectrum of non-loaded OSA-HA nanogels was obtained at a concentration of 0.4 mg/mL (Supporting information, Figure S2). Spectra (n = 3) were recorded in the range 190–260 nm (1 nm resolution) at 25 °C, corrected for background contributions.

Release of DJK-5 from nanogels

In vitro release studies were performed in HEPES buffer (10 mM, pH 7.4) with the ionic strength adjusted by addition of 150 mM NaCl. Briefly, nanogel dispersions were diluted to 1 mg/mL of DJK-5 in water and added to a dialysis tube (Spectra-Por® Float-a-Lyzer® G2, MWCO 100 kDa, Spectrum Labs, Breda, the Netherlands) and placed in the release buffer stirred with a magnetic stirrer at 250 rpm. The temperature was maintained at 37 °C in an INNUCELL incubator (MMM Medcenter Einrichtungen, Munich, Germany) throughout the experiment. Studies were conducted in triplicates on independent batches of nanogels.

In vivo peptide compatibility studies

All animal experiments were performed in accordance with The Canadian Council on Animal Care (CCAC) guidelines and were approved by the University of British Columbia Animal Care Committee (certificate number A14-0363). Mice used in this study were female outbred CD-1. All animals were purchased from Charles River Laboratories (Wilmington, MA, USA), were 7 weeks of age, and weighed about 25 ± 3 g at the time of the experiments. The mice were anaesthetized using 1 to 3% isoflurane and euthanized with carbon dioxide.

Toxicity *in vivo* was assessed as previously described [27]. Briefly, the fur on the backs of the mice was removed by shaving and application of chemical depilatories. Freshly prepared nanogel

formulations (50 µL) in endotoxin-free water were injected subcutaneously into the right side of the dorsum underneath the thin skeletal muscle. The non-formulated peptide DJK-5 was initially dissolved in endotoxin-free water and further diluted in saline for *in vivo* application. After 24 h, the animals were sacrificed and the epithelial tissue damage caused by the nanogels was evaluated by visual assessment of the injection area.

For evaluation of systemic toxicity after intravenous injection, mice (n=5-7 per group) received a 100 µL tail vein injection of either 1.5 mg/mL non-formulated DJK-5 in saline, 3.5 mg/mL non-formulated DJK-5 in saline, 3 mg/mL of DJK-5 in nanogels or 6 mg/mL DJK-5 in nanogels. In addition, a group of mice (n=2) received a tail vein injection of peptide-free nanogels (20 mg/mL OSA-HA polymer corresponding to the amount of polymer dosed in the 6 mg/mL nanogels). All nanogels were administered 1-2 h after formulation of the OSA-HA polymer with the peptide DJK-5. Systemic toxicity was evaluated 30 min after injection, by visual assessment of animal viability (lethality of the injection).

Cutaneous mouse infection model

The abscess infection model was performed as described earlier [13,27]. For the experiment, the fur on the backs of the mice was removed by shaving and application of chemical depilatories. *P. aeruginosa* LESB58 [28] was grown to an OD_{600} of 1.0 in double yeast tryptone broth. Prior to injection, bacterial cells were washed twice with sterile phosphate-buffered saline (PBS) and adjusted to 5×10^7 CFU/mL. A 50 µL bacterial suspension was injected subcutaneously into the right side of the dorsum. Peptide concentrations for efficacy testing were 1.5 mg/mL for DJK-5 dissolved in saline, as well as 3- and 6 mg/mL DJK-5 encapsulated in nanogel. Peptides, saline, or nanogel (50 µL) were directly injected subcutaneously into the infected area *via* intra-abscess injection at 1 h post infection.

The progression of the disease/infection was monitored daily and abscess lesion sizes on day three were measured using a caliper. Swelling/inflammation was not considered in the measurements. Skin abscesses were excised (including all accumulated pus), homogenized in sterile PBS using a Mini-Beadbeater-96 (BioSpec Products, Bartlesville, OK, USA) for 5 min and bacterial counts determined by serial dilution.

Quantification of reactive oxygen species and reactive nitrogen species (ROS/RNS)

The detection of ROS/RNS production was carried out as previously described [27]. Briefly, L-012, a chemiluminescence probe [29], was injected subcutaneously (12.5 mg/mL) between the ears of the mice one hour after intra-abscess administration of 1.5 or 3.5 mg/mL non-formulated DJK-5, non-loaded nanogels (10- or 20 mg/mL OSA-HA, corresponding to the polymer concentration in nanogels loaded with 3 mg/mL and 6 mg/mL DJK-5, respectively) or nanogel formulations containing 3 or 6 mg/mL of DJK-5. Representative images were acquired using a Lumina *in vivo* imaging system (IVIS, 60 s exposure, medium binning) and analyzed using Living Image software (Perkin Elmer, Waltham, MA, USA).

Statistical analysis

For *in vitro* studies, three independent experiments were conducted and are presented as mean ± standard deviation (SD). Statistical evaluations of *in vivo* experiments were performed using GraphPad Prism 6.0 (GraphPad Software, La Jolla, CA, USA). P values (* $p<0.05$; ** $p<0.01$) were calculated using a two-tailed unpaired Student's t-test. For all animal experiments, the number of biological replicates is indicated in the Figure legend.

Results

Physicochemical characteristics of the nanogels

Nanogels encapsulating DJK-5 were prepared with varying concentrations of DJK-5, but at the same peptide to polymer ratio of 0.3:1, resulting in a satisfactory formation of nanogels. The size, PDI, ZP and EE of DJK-5 for the prepared nanogels are presented in Table 1.

The more neutral ZP of the DJK-5-loaded nanogels in comparison to non-loaded nanogels confirmed the presence of surface-bound peptide and/or peptide encapsulated in nanogels. Negative staining of the nanogels together with TEM imaging confirmed the presence of individual spherical nanogel structures (Figure 1). The presence of very small nanogels in addition to nanogels of approximately 200 nm (Figure 1A) could be observed for the non-loaded nanogels, in contrast to nanogels encapsulating DJK-5 which had a more homogenous size distribution (Figures 1B, C). This was in accordance with the slightly higher PDI values obtained from dynamic light scattering measurements for the non-loaded nanogels as compared to those of the loaded nanogels (Table 1). Importantly, the size of a particle population measured using dynamic light scattering is presented as Z-average, a single number that is an intensity based harmonic mean based on the whole sample population, whereas TEM displays only a very small part of the whole population.

Circular dichroism studies were performed to confirm the association of DJK-5 with the OSA-HA polymer upon formation of the nanogels. As hydrophobic moieties in close proximity to peptides induce conformational changes in the peptide [30], we expect that close proximity to the hydrophobic OSA side chain (attached to the HA backbone) to the peptide will induce folding in a similar manner. Indeed, a change in secondary structure from unstructured to structured DJK-5 was observed indicating interactions between the peptide molecules and the polymer in the formulation (Figure 2). Interestingly, the secondary structure was maintained upon release and separation of DJK-5 from the nanogels (Supplementary results, Figure S1).

The nanogels showed good stability when stored in ultrapure water at 4°C, with no leakage of peptide over 24 h (Supplementary results, Figure S2). Approximately 80% of DJK-5 was released in isoosmolar buffer from all nanogel formulations within the first 5 h and almost complete release of peptide was obtained within 48 h (Figure 3). As HA is degraded by hyaluronidase in the body, the enzymatic degradation of non-modified HA and OSA-HA was assessed, and the results indicate that the modification of HA with OSA increases enzymatic stability of the polymer (Supplementary results, Figure S3). However, hyaluronidase-triggered release of the peptide from the nanogels showed only a tendency towards a slight increase in peptide release over 48h, in comparison to release in isoosmolar buffer (Supplementary results, Figure S4).

In vivo toxicity of DJK-5 in nanogels

The peptide DJK-5 has been shown to be effective for treatment of bacterial abscesses [13] but caused tissue damage *in vivo* at concentrations above 1.5 mg/mL (Supplementary results, Figure S5). Peptide toxicity *in vivo* was assessed for the peptide formulated in nanogels to deliver 3-, 4.5-, 6- and 7.5 mg/mL DJK-5. No obvious signs of inflammation or tissue necrosis were observed for nanogels containing up to 6 mg/mL of DJK-5. However, at 7.5 mg/mL of DJK-5 in nanogels, inflammation was evident (Figure 4), and as a result these nanogels were excluded from further studies. Overall, this shows that the dose of DJK-5 that can be administered intra-abscess could be increased from 1.5 mg/mL to 6 mg/mL without inducing significant tissue toxicity. No notable differences were observed between the nanogel formulations in terms of e.g., size, ZP and DJK-5 release kinetics and therefore the nanogels containing a low (3 mg/mL) and high (6 mg/mL) concentration of DJK-5 were chosen for *in vivo* performance assessment. However, it should be noted that whereas the nanogels with 3- and 4.5 mg/mL DJK-5 were clear, a slight change in turbidity was observed in the nanogel formulations containing 6- and 7.5 mg/mL of DJK-5,

indicating slight aggregation. This could explain the inflammation observed after dosing 7.5 mg/mL.

To investigate the possibility of using nanogel formulations for systemic delivery, the nanogel dispersions were administered intravenously to mice *via* tail vein injection and animal survival 30 min post injection was evaluated (Supplementary results, Figure S6). No mortality was observed among mice exposed to the injection of 3 mg/mL nanogel formulation (n=5), in contrast to 1.5 mg/mL non-formulated DJK-5, which was lethal in 50% of the test population (n=6). Nanogels containing 6 mg/mL DJK-5 were also lethal in approximately 50% of the test group (n=7). No mortality was observed in the group (n=2) treated with non-loaded nanogels.

An important part of the inflammatory response in host defence is the production of reactive oxygen species (ROS) and reactive nitrogen species (RNS) by phagocytic cells [29]. ROS/RNS production was observed after administration of nanogels containing DJK-5 (Figure 5). This increase was not observed in mice treated with non-loaded nanogels or non-formulated DJK-5. The increased production of ROS/RNS may be due to an influx and activation of phagocytic cells producing reactive species, though the exact cause is unclear.

Efficacy in reducing subcutaneous abscesses

Nanogels with 3 mg/mL and with 6 mg/mL were investigated further in efficacy studies using the murine *P. aeruginosa* LESB58 abscess model [13,27]. The formulations were administered via intra-abscess injection, 1 h post infection. Both nanogel formulations significantly decreased the abscess size as compared to the non-loaded nanogels (Figure 6A), but resulted in a similar decrease in abscess size when compared to treatment with a solution of 1.5 mg/mL DJK-5. The bacterial load recovered from the abscesses treated with the DJK-5-loaded nanogels was significantly lowered,

approximately 4-fold compared to the non-loaded nanogel controls (Figure 6B). To further investigate the antimicrobial activity of DJK-5 and DJK-5 in nanogels, minimum inhibitory concentration (MIC) determination and time-kill studies were performed on *P. aeruginosa* PAO1 (Supplementary results, Figures S7 and S8). We observed that the MIC for DJK-5 increased by 1-fold dilution upon encapsulation in nanogels (Supplementary material, page 7). DJK-5 eradicated *P. aeruginosa* within 5 h at MIC as well as concentrations above MIC in a similar manner, suggesting a time-dependent killing profile towards *P. aeruginosa* PAO1 (Supplementary results, Figure S6). The DJK-5-loaded nanogels at 64 µg/mL presented a bacteriostatic effect for 5 h and subsequent regrowth of the bacterial colony after 24 h, similar to non-formulated DJK-5 at the same concentration (Supplementary results, Figure S7).

Discussion

The worldwide spread of antimicrobial resistance has increased the interest in the development of novel antimicrobial agents [31,32] such as antimicrobialAMPs and anti-biofilm peptides. Although multiple mechanisms of killing have been described for AMPs [33], the most frequently reported mechanism of action occurs due to the physicochemical properties of AMPs; their overall positive charge and amphipathicity allow binding to bacterial surface and membrane disruption through pore formation. The fast bacterial killing caused by membrane disruption creates an advantage for AMPs, as development of resistance through gene mutations is lower than compared to traditional antibiotics [34,35]. However, some peptides show low cell specificity, while others aggregate [36], resulting in undesirable host toxicity during treatment [37,38]. These side effects can be overcome by using drug delivery systems such as nanogels. Here, we describe the *in vivo* application of a nanogel formulation with the overall aim to increase the compatibility of DJK-5. Nanogels encapsulating 2-, 3-, 4.5-, 6- and 7.5 mg/mL of DJK-5 were prepared and characterized. Particles in

the size range of 174-194 nm were formed and were of similar size as previously reported nanoparticles composed of 234 kDa HA modified with cholesterol [39] and nanoparticles composed of ceramide-modified 4.7 kDa HA [40]. However, in this study, the PDI indicated moderate to high polydispersity of the nanogel populations, which was confirmed using TEM. It is likely that preparation of the DJK-5 nanogels using bulk mixing caused such high PDI, as OSA-HA nanogels prepared using microfluidics-assisted self-assembly showed a lower PDI [26]. All nanogels showed a more neutral ZP than non-loaded nanogels, suggesting the presence of surface-bound or encapsulated peptide, in accordance with previous reports [41]. Upon encapsulation of DJK-5 in nanogels, a slight decrease in particle size of the nanogels was observed, a typical behaviour for loaded nanogels [42]. The encapsulation efficiency of DJK-5 into OSA-HA nanogels was relatively low in comparison to peptoid-loaded OSA-HA nanogels [26], where the encapsulation efficiency reached 90%. Generally, higher encapsulation efficiency can be obtained for nanogels in comparison to other delivery systems such as polymeric micelles or liposomes [42], but the peptide loading into nanogels will depend on multiple parameters, including peptide length [43], hydrophobicity [44], charge, and secondary structure [45]. The change in secondary structure of DJK-5 upon encapsulation within the hydrophobic areas of the nanogels is consistent with previous reports, which suggest that presence of peptides in close proximity to hydrophobic moieties induces conformational changes of the peptide [30]. To exert its activity, the peptide must be released from the carrier and fold upon interaction with the bacterial membranes [46]. We have observed that the peptide retained its folded secondary structure after release from the nanogels, likely due to the presence of unbound lipid (OSA) side chains remaining in the OSA-HA sample.

The nanogels showed good stability in ultrapure water at 4°C, with a small increase in DJK-5 encapsulation over time, as previously reported [47]. Release of encapsulated compound from loosely-bound nanogels such as OSA-HA nanogels is thought to be triggered by the presence of

electrolytes, which lead to disentanglement of the polymer chains [25,48] but also through degradation of HA backbone. We have assessed the enzymatic activity of hyaluronidase towards HA and OSA-HA and observed increased enzymatic stability of the modified polymer, consistent with literature [49]. The release of DJK-5 triggered by presence of hyaluronidase showed only a slight increase in peptide release from the nanogels, in addition to the 80% release of DJK-5 obtained for all nanogel formulations in medium iso-osmolar to blood plasma within 5 hours. The fast release of DJK-5 may also indicate that the peptide was located close to the surface of the nanogels, as has been previously reported for hyaluronic acid-based nanoparticles encapsulating siRNA [39]. Ion-triggered release will not be applicable for all modified HA nanoparticles and the release trigger will depend on the modification. Nanogels composed of riboflavin-modified 200 kDa HA showed stability in isotonic medium for 15 days [50], whereas nanoparticles composed of cholesterol-modified 234 kDa HA showed stability in PBS for 6 days and drug release in acidic conditions [39]. Slow (1.7% daily) sustained release from cholesteryl-modified 62 kDa HA nanogel-drug conjugates due to hydrolysis of the ester linkage has also been reported [51].

The high EE together with the negative surface charge of nanogels are parameters that are expected to improve the safety of AMPs as positive charges and hydrophobic regions which favor aggregation of peptides have previously been correlated with increased hemolysis and cytotoxicity towards eukaryotic cells [11,12]. Improved safety in the use of such cationic peptides was confirmed in our studies since the amount of DJK-5 that could be administered subcutaneously without causing toxicity *in vivo* was increased four-fold upon encapsulation in nanogels. Even upon intravenous injection, 3 mg/mL DJK-5 in nanogels, which contained approximately 2 mg/mL unbound peptide present in the supernatant with the nanogels (Table 1), could be administered without adverse side effects, compared to 1.5 mg/mL of non-formulated DJK-5 which was lethal in half of the murine test population. Improving the compatibility of intravenously administered AMPs

and anti-biofilm peptides would allow for broader applications of such peptides, including the intravenous treatment of severe infections, such as bacteremia [52], endocarditis [53] or diabetic foot ulcers [54]. The use of AMPs such as gramidicin S and polymyxin B is currently limited to topical applications due to systemic toxicity [55–57]. However, colistimethate sodium, a prodrug of polymyxin, significantly reduces toxicity of this peptide and allows administration *via* intravenous and inhalation routes [58].

Host immune cells such as neutrophils release high concentrations of ROS after activation of surface receptors, and high ROS concentrations are known to support clearance of invading pathogens [59]. The increase in ROS/RNS production observed in mice exposed to both 3- and 6 mg/mL DJK-5 encapsulated in nanogels may be a result of increased presence of neutrophils at the injection site triggered by the drug-loaded nanogel formulations, possibly indicating an immunostimulatory effect of these treatments.

Infections with *P. aeruginosa* LESB58 cause localized high bacterial density skin and soft tissue infections for up to 10 days without inducing systemic infection [27]. One hour post infection, the abscesses were treated via intra-abscess injection with DJK-5 or DJK-5-loaded nanogel formulations. Intra-abscess injections are not suitable for clinical treatment of such infections, but reflect local administration of antimicrobials and provide crucial understanding on the peptide dose needed to decrease such infections. The efficacy of both nanogel treatments (3- and 6 mg/mL) was similar to 1.5 mg/mL non-formulated DJK-5. The time-dependent killing profile of DJK-5 after encapsulation in nanogels may explain why no additional reduction of abscess size and bacterial load was observed after administration of four-fold higher concentrations of DJK-5 in nanogels. Importantly, DJK-5 is not an AMP; therefore additional reduction of bacterial load upon administration of higher doses of the peptide is not anticipated.

Overall, the hypothesis that the OSA-HA nanogel formulation could reduce the toxicity associated with *in vivo* administration of DJK-5 without significantly affecting the efficacy of the non-formulated peptide dose was confirmed. Self-assembly of peptides and OSA-HA into nanogels may be a successful formulation approach for reducing the toxicity of antimicrobial and anti-biofilm peptides and allow for further development of these peptides into a commercial anti-biofilm or anti-abscess agents. The moderate (33-60%) encapsulation efficiency of DJK-5 into OSA-HA nanogels may seem to be a limiting step in the advancement of DJK-5-loaded OSA-HA nanogels into a therapeutic agent. However, as mentioned above, loading peptides into nanogels is in general considered high compared to other colloidal drug delivery systems and the process conditions should certainly be optimized when upscaling to achieve the highest possible encapsulation. Additionally, more tailored nanogel systems and various formulation conditions should be explored to find the most suitable delivery system for DJK-5 and allow its efficient use in the clinic.

Acknowledgments

The authors acknowledge the Core Facility for Integrated Microscopy, Faculty of Health and Medical Sciences, University of Copenhagen for their help with the TEM images.

References

[1] M.S. Dryden, Complicated skin and soft tissue infection, J. Antimicrob. Chemother. 65 (2010) 35–44. doi:10.1093/jac/dkq302.

[2] R. Mistry, D. Shapiro, M. Goyal, T. Zaoutis, J. Gerber, C. Liu, A. Hersh, Clinical management of skin and soft tissue infections in the U.S. emergency departments, West. J. Emerg. Med. 15 (2014) 491–498. doi:10.5811/westjem.2014.4.20583.

[3] C. Ruef, Complicated skin and soft-tissue infections – consider Gram-negative pathogens, Infection. 36 (2008) 295. doi:10.1007/s15010-008-3408-8.

[4] K. Gjødsbøl, J.J. Christensen, T. Karlsmark, B. Jørgensen, B.M. Klein, K.A. Krogfelt, Multiple bacterial species reside in chronic wounds: A longitudinal study, Int. Wound J. 3 (2006) 225–231. doi:10.1111/j.1742-481X.2006.00159.x.

[5] P.D. Lister, D.J. Wolter, N.D. Hanson, Antibacterial-resistant Pseudomonas aeruginosa: Clinical impact and complex regulation of chromosomally encoded resistance mechanisms, Clin. Microbiol. Rev. 22 (2009) 582–610. doi:10.1128/CMR.00040-09.

[6] G. Batoni, G. Maisetta, S. Esin, Antimicrobial peptides and their interaction with biofilms of medically relevant bacteria, Biochim. Biophys. Acta - Biomembr. 1858 (2016) 1044–1060. doi:10.1016/j.bbamem.2015.10.013.

[7] S.C. Mansour, C. De La Fuente-Núñez, R.E.W. Hancock, Peptide IDR-1018: modulating the immune system and targeting bacterial biofilms to treat antibiotic-resistant bacterial infections, J. Pept. Sci. 21 (2015) 323–329. doi:10.1002/psc.2708.

[8] K.A. Brogden, Antimicrobial peptides: pore formers or metabolic inhibitors in bacteria?, Nat. Rev. Microbiol. 3 (2005) 238–250. doi:10.1038/nrmicro1098.

[9] C. de la Fuente-Núñez, R.E.W. Hancock, Using anti-biofilm peptides to treat antibiotic-resistant bacterial infections, Postdoc J. 3 (2015) 1–8. doi:10.14304/SURYA.JPR.V3N2.1.

[10] C. De La Fuente-Núñez, F. Reffuveille, S.C. Mansour, S.L. Reckseidler-Zenteno, D. Hernández, G. Brackman, T. Coenye, R.E.W. Hancock, D-enantiomeric peptides that eradicate wild-type and multidrug-resistant biofilms and protect against lethal Pseudomonas aeruginosa infections, Chem. Biol. 22 (2015) 196–205. doi:10.1016/j.chembiol.2015.01.002.

[11] J.S. Bahnsen, H. Franzyk, A. Sandberg-Schaal, H.M. Nielsen, Antimicrobial and cell-penetrating properties of penetratin analogs: effect of sequence and secondary structure, Biochim. Biophys. Acta - Biomembr. 1828 (2013) 223–232. doi:10.1016/j.bbamem.2012.10.010.

[12] Z. Jiang, A.I. Vasil, J.D. Hale, R.E.W. Hancock, M.L. Vasil, R.S. Hodges, Effects of net charge and the number of positively charged residues on the biological activity of amphipathic alpha-helical cationic antimicrobial peptides, Biopolymers. 90 (2008) 369–383. doi:10.1002/bip.20911.

[13] S.C. Mansour, D. Pletzer, C. de la Fuente-Núñez, P. Kim, G.Y.C. Cheung, H.S. Joo, M. Otto, R.E.W. Hancock, Bacterial abscess formation is controlled by the stringent stress response and can be targeted therapeutically, EBioMedicine. 12 (2016) 219–226. doi:10.1016/j.ebiom.2016.09.015.

[14] D. Pletzer, H. Wolfmeier, M. Bains, R.E.W. Hancock, Synthetic peptides to target stringent response-controlled virulence in a Pseudomonas aeruginosa murine cutaneous infection model, Front. Microbiol. 8 (2017) 1–15. doi:10.3389/fmicb.2017.01867.

[15] D. Pletzer, S.C. Mansour, R.E.W. Hancock, Synergy between conventional antibiotics and anti-biofilm peptides in a murine, sub-cutaneous abscess model caused by recalcitrant ESKAPE pathogens, PLoS Pathog. 14 (2018) e1007084. doi:10.1371/journal.ppat.1007084.

[16] P. Almeida, Membrane-active peptides: binding, translocation, and flux in lipid vesicles, Biochim Biophys Acta. 1838 (2014) 2216–2227.

doi:10.1016/j.bbamem.2014.04.014.Membrane-active.

[17] J.P. Silva, C. Gonçalves, C. Costa, J. Sousa, R. Silva-Gomes, A.G. Castro, J. Pedrosa, R. Appelberg, F.M. Gama, Delivery of LLKKK18 loaded into self-assembling hyaluronic acid nanogel for tuberculosis treatment, J. Control. Release. 235 (2016) 112–124. doi:10.1016/j.jconrel.2016.05.064.

[18] J.J. Water, Y. Kim, M.J. Maltesen, H. Franzyk, C. Foged, H.M. Nielsen, Hyaluronic acid-based nanogels produced by microfluidics-facilitated self-assembly improves the safety profile of the cationic host defense peptide novicidin, Pharm. Res. (2015) 2727–2735. doi:10.1007/s11095-015-1658-6.

[19] H. Zhang, Y. Zhai, J. Wang, G. Zhai, New progress and prospects: The application of nanogel in drug delivery, Mater. Sci. Eng. C. 60 (2016) 560–568. doi:10.1016/j.msec.2015.11.041.

[20] S. Manchun, C.R. Dass, P. Sriamornsak, Stability of freeze-dried pH-responsive dextrin nanogels containing doxorubicin, Asian J. Pharm. Sci. 11 (2016) 648–654. doi:10.1016/j.ajps.2015.09.006.

[21] N. Morimoto, T. Ohki, K. Kurita, K. Akiyoshi, Thermo-responsive hydrogels with nanodomains: rapid shrinking of a nanogel-crosslinking hydrogel of poly(N-isopropyl acrylamide), Macromol. Rapid Commun. 29 (2008) 672–676. doi:10.1002/marc.200700864.

[22] C. Eenschooten, F. Guillaumie, G.M. Kontogeorgis, E.H. Stenby, K. Schwach-Abdellaoui, Preparation and structural characterisation of novel and versatile amphiphilic octenyl succinic anhydride-modified hyaluronic acid derivatives, Carbohydr. Polym. 79 (2010) 597–605. doi:10.1016/j.carbpol.2009.09.011.

[23] C. Eenschooten, Development of soft nanocarriers from novel amphiphilic hyaluronic acid derivatives towards drug delivery, 2008. ISBN-13: 978-87-91435-84-6.

[24] C. Eenschooten, A. Vaccaro, F. Delie, F. Guillaumie, K. Tømmeraas, G.M. Kontogeorgis, K. Schwach-Abdellaoui, M. Borkovec, R. Gurny, Novel self-associative and multiphasic nanostructured soft carriers based on amphiphilic hyaluronic acid derivatives, Carbohydr. Polym. 87 (2012) 444–451. doi:10.1016/j.carbpol.2011.08.004.

[25] K. Tømmeraas, M. Mellergaard, B.M. Malle, P. Skagerlind, New amphiphilic hyaluronan derivatives based on modification with alkenyl and aryl succinic anhydrides, Carbohydr. Polym. 85 (2011) 173–179. doi:10.1016/j.carbpol.2011.02.011.

[26] S. Kłodzińska, N. Molchanova, H. Franzyk, P. Robert Hansen, P. Damborg, H. Mørck Nielsen, Biopolymer nanogels improve antibacterial activity and safety profile of a novel lysine-based α-peptide/β-peptoid peptidomimetic, Eur. J. Pharm. Biopharm. 128 (2018) 1–9. doi:10.1016/j.ejpb.2018.03.012.

[27] D. Pletzer, S.C. Mansour, K. Wuerth, N. Rahanjam, R.E.W. Hancock, New mouse model for chronic infections by Gram-negative bacteria enabling the study of anti-infective efficacy and host-microbe interactions, MBio. 8 (2017) e00140–17.

[28] K. Cheng, R.L. Smyth, J.R.W. Govan, C. Doherty, C. Winstanley, N. Denning, D.P. Heaf, H. Van Saene, C.A. Hart, Spread of β-lactam-resistant Pseudomonas aeruginosa in a cystic fibrosis clinic, Lancet. 348 (1996) 639–642. doi:10.1016/S0140-6736(96)05169-0.

[29] A. Kielland, T. Blom, K.S. Nandakumar, R. Holmdahl, R. Blomhoff, H. Carlsen, In vivo imaging of reactive oxygen and nitrogen species in inflammation using the luminescent probe L-012, Free Radic. Biol. Med. 47 (2009) 760–766. doi:10.1016/j.freeradbiomed.2009.06.013.

[30] R. Zhang, T. Eckert, T. Lutteke, S. Hanstein, A. Scheidig, A. M. J. J. Bonvin, N. E. Nifantiev, T. Kozar, R. Schauer, M. Abdulaziz Enani, H.-C. Siebert, Structure-function relationships of antimicrobial peptides and proteins with respect to contact molecules on

pathogen surfaces, Curr. Top. Med. Chem. 16 (2016) 89–98. doi:10.2174/1568026615666150703120753.

[31] M. Pasupuleti, A. Schmidtchen, M. Malmsten, Antimicrobial peptides: key components of the innate immune system, Crit. Rev. Biotechnol. 32 (2012) 143–171. doi:10.3109/07388551.2011.594423.

[32] R.E.W. Hancock, H.-G. Sahl, Antimicrobial and host-defense peptides as new anti-infective therapeutic strategies, Nat. Biotechnol. 24 (2006) 1551–1557. doi:10.1038/nbt1267.

[33] L.T. Nguyen, E.F. Haney, H.J. Vogel, The expanding scope of antimicrobial peptide structures and their modes of action, Trends Biotechnol. 29 (2011) 464–472. doi:10.1016/j.tibtech.2011.05.001.

[34] R.D. Jahnsen, E.F. Haney, H. Franzyk, R.E.W. Hancock, Characterization of a proteolytically stable multifunctional host defense peptidomimetic, Chem. Biol. 20 (2013) 1286–1295. doi:10.1016/j.chembiol.2013.09.007.

[35] A. Peschel, H.G. Sahl, The co-evolution of host cationic antimicrobial peptides and microbial resistance, Nat. Rev. Microbiol. 4 (2006) 529–536. doi:10.1038/nrmicro1441.

[36] E.F. Haney, B. (Catherine) Wu, K. Lee, A.L. Hilchie, R.E.W. Hancock, Aggregation and its influence on the immunomodulatory activity of synthetic innate defense regulator peptides, Cell Chem. Biol. 24 (2017) 969–980. doi:10.1016/j.chembiol.2017.07.010.

[37] Y. Chen, C.T. Mant, S.W. Farmer, R.E.W. Hancock, M.L. Vasil, R.S. Hodges, Rational design of alpha-helical antimicrobial peptides with enhanced activities and specificity/therapeutic index, J. Biol. Chem. 280 (2005) 12316–12329. doi:10.1074/jbc.

[38] S. Maher, S. McClean, Investigation of the cytotoxicity of eukaryotic and prokaryotic antimicrobial peptides in intestinal epithelial cells in vitro, Biochem. Pharmacol. 71 (2006) 1289–1298. doi:10.1016/j.bcp.2006.01.012.

[39] K. Choi, M. Jang, J.H. Kim, H.J. Ahn, Tumor-specific delivery of siRNA using supramolecular assembly of hyaluronic acid nanoparticles and 2b RNA-binding protein/siRNA complexes, Biomaterials. 35 (2014) 7121–7132. doi:10.1016/j.biomaterials.2014.04.096.

[40] H.-J. Cho, I.-S. Yoon, H.Y. Yoon, H. Koo, Y.-J. Jin, S.-H. Ko, J.-S. Shim, K. Kim, I.C. Kwon, D.-D. Kim, Polyethylene glycol-conjugated hyaluronic acid-ceramide self-assembled nanoparticles for targeted delivery of doxorubicin, Biomaterials. 33 (2012) 1190–1200. doi:10.1016/j.biomaterials.2011.10.064.

[41] A.T. Press, A. Ramoji, M. vd Lühe, A.C. Rinkenauer, J. Hoff, M. Butans, C. Rössel, C. Pietsch, U. Neugebauer, F.H. Schacher, M. Bauer, Cargo–carrier interactions significantly contribute to micellar conformation and biodistribution, NPG Asia Mater. 9 (2017) e444. doi:10.1038/am.2017.161.

[42] A. V Kabanov, S. V. Vinogradov, Nanogels as pharmaceutical carriers: finite networks of infinite capabilities, Angew Chem Int Ed Engl. 48 (2009) 5418–5429. doi:10.1002/anie.200900441.Nanogels.

[43] L. Nyström, R. Nordström, J. Bramhill, B.R. Saunders, R. Álvarez-Asencio, M.W. Rutland, M. Malmsten, Factors affecting peptide interactions with surface-bound microgels, Biomacromolecules. 17 (2016) 669–678. doi:10.1021/acs.biomac.5b01616.

[44] H. Bysell, P. Hansson, A. Schmidtchen, M. Malmsten, Effect of hydrophobicity on the interaction between antimicrobial peptides and poly(acrylic acid) microgels, J. Phys. Chem. B. 114 (2010) 1307–1313. doi:10.1021/jp910068t.

[45] R. Månsson, H. Bysell, P. Hansson, A. Schmidtchen, M. Malmsten, Effects of peptide secondary structure on the interaction with oppositely charged microgels, Biomacromolecules. 12 (2011) 419–424. doi:10.1016/j.colsurfa.2011.01.029.

[46] C. Avitabile, L.D. D'Andrea, A. Romanelli, Circular dichroism studies on the interactions of antimicrobial peptides with bacterial cells, Sci. Rep. 4 (2014) 1–7. doi:10.1038/srep04293.

[47] K.T. Oh, T.K. Bronich, V.A. Kabanov, A. V. Kabanov, Block polyelectrolyte networks from poly(acrylic acid) and poly(ethylene oxide): sorption and release of cytochrome C, Biomacromolecules. 8 (2007) 490–497. doi:10.1021/bm060599g.

[48] S. Furlan, G. La Penna, A. Perico, A. Cesàro, Hyaluronan chain conformation and dynamics, Carbohydr. Res. 340 (2005) 959–970. doi:10.1016/j.carres.2005.01.030.

[49] C.-H. Wong, Chapter 15: Chemistry, biochemistry, and pharmaceutical potentials of glycosaminoglycans and related saccharides., in: Carbohydrate-Based Drug Discov., 2003: pp. 407–433.

[50] C. Di Meo, E. Montanari, L. Manzi, C. Villani, T. Coviello, P. Matricardi, Highly versatile nanohydrogel platform based on riboflavin-polysaccharide derivatives useful in the development of intrinsically fluorescent and cytocompatible drug carriers, Carbohydr. Polym. 115 (2015) 502–509. doi:10.1016/j.carbpol.2014.08.107.

[51] X. Wei, T. Senanayake, G. Warren, S. Vingradov, Hyaluronic acid-based nanogel-drug conjugates with enhanced anticancer activity designed for targeting of CD44-positive and drug-resistant tumors, Bioconjug. Chem. 24 (2013) 658–668. doi:10.1111/j.1743-6109.2008.01122.x.Endothelial.

[52] J.R. Shiu, E. Wang, A.M. Tejani, M. Wasdell, Continuous versus intermittent infusions of antibiotics for the treatment of severe acute infections, Cochrane Database Syst. Rev. (2013) CD008481. doi:10.1002/14651858.CD008481.pub2.www.cochranelibrary.com.

[53] B. Hoen, Epidemiology and antibiotic treatment of infective endocarditis: an update, Heart. 92 (2006) 1694–1700. doi:10.1136/hrt.2005.072595.

[54] A. Selva Olid, I. Solà, L.A. Barajas-Nava, O. Gianneo, X. Bonfill Cosp, B.A. Lipsky,

Systemic antibiotics for treating diabetic foot infections, Cochrane Database Syst. Rev. (2015) CD009061. doi:10.1002/14651858.CD009061.pub2.www.cochranelibrary.com.

[55] R. Mösges, C.M. Baues, T. Schröder, K. Sahin, Acute bacterial otitis externa: efficacy and safety of topical treatment with an antibiotic ear drop formulation in comparison to glycerol treatment, Curr. Med. Res. Opin. 27 (2011) 871–878. doi:10.1185/03007995.2011.557719.

[56] N. Molchanova, P.R. Hansen, H. Franzyk, Advances in development of antimicrobial peptidomimetics as potential drugs, Molecules. 22 (2017) 1430. doi:10.3390/molecules22091430.

[57] F. Rabanal, Y. Cajal, Recent advances and perspectives in the design and development of polymyxins, Nat. Prod. Rep. 34 (2017) 886–908. doi:10.1039/C7NP00023E.

[58] M.E. Falagas, S.K. Kasiakou, Toxicity of polymyxins: A systematic review of the evidence from old and recent studies, Crit. Care. 10 (2006) R27. doi:10.1186/cc3995.

[59] G.T. Nguyen, E.R. Green, J. Mecsas, Neutrophils to the ROScue: mechanisms of NADPH oxidase activation and bacterial resistance, Front. Cell. Infect. Microbiol. 7 (2017) 373. doi:10.3389/fcimb.2017.00373.

Table 1**.** Nanogels prepared for efficacy assessment.

Figure 1. Negative stain TEM images of A) non-loaded nanogels (10 mg/mL OSA-HA), and nanogels loaded with B) 3 mg/mL of DJK-5, and C) 6 mg/mL of DJK-5. Yellow arrows indicate individual nanogels. Scale bar indicates 1 µm.

Figure 2. Superimposition of circular dichroism spectra of non-formulated DJK-5 in ultrapure water (▬ ▬) and of nanogels; 2 mg/mL nanogels (▬), 3 mg/mL nanogels (▬), 4.5 mg/mL nanogels (▬), 6 mg/mL nanogels (▬), and 7.5 mg/mL nanogels (▬) containing DJK-5. DJK-5 is a D-form peptide, thus spectra are mirror images of those which would be obtained for an L-form of this peptide. All spectra were obtained at a peptide concentration of 0.125 mg/mL. Representative spectra, n = 3.

Figure 3. Accumulated release of DJK-5 relative to the total amount from 2 mg/mL nanogels (●), 3 mg/mL nanogels (■), 4.5 mg/mL nanogels (▲), 6 mg/mL nanogels (▼), and 7.5 mg/mL nanogels (◆) in HEPES buffer (10 mM, pH 7.4) with ionic strength adjusted to 150 mM with NaCl. n = 3 ± SD, except 7.5 mg/mL nanogels, where n = 2 ± SD.

Figure 4. Representative images of skin appearance from the epidermis (left) and hypodermis (right) sides 24 h post injection of nanogels containing DJK-5. No signs of inflammation were visible at concentrations up to 6 mg/mL. At 7.5 mg/mL inflammation of the hypodermis was observed (circled in yellow), n = 3 – 5 per group.

Figure 5. *In vivo* tracking of ROS and RNS production. ROS/RNS production was measured 1 h after treatment injection. The described left or right side is based on the position of the tail from the

top view. A) Non-loaded nanogels corresponding to the concentration of OSA-HA in 3 mg/mL and 6 mg/mL DJK-5-loaded nanogels, respectively (Table 1): 10 mg/ml OSA-HA (left) and 20 mg/ml OSA-HA (right), B) 1.5 mg/mL non-formulated DJK-5 (left) and 3 mg/mL DJK-5 in nanogels (right), C) 3.5 mg/mL non-formulated DJK-5 (left) and 6 mg/mL DJK-5 in nanogels (right). Representative images are shown (n = 3 – 6 per group). Mice were imaged using an *in vivo* imaging system (IVIS) and luminescence intensity of photons is presented.

Figure 6. Therapeutic treatment of mouse cutaneous abscesses. Mice infected subcutaneously with *P. aeruginosa* LESB58 were treated with intra-abscess administration of saline, 1.5 mg/mL of DJK-5 in saline, non-loaded nanogels and two DJK-5 nanogel formulations 1 hour post infection. A) Lesions were measured 72 h post-infection using a caliper. Representative images of abscesses treated with each type of treatment are shown above the graph. B) The number of bacteria recovered from abscesses infected with *P. aeruginosa* LESB58 72 hours post-infection, and plated for enumeration. Experiments were performed three times, n = 9 – 14 animals per group.

The antibiofilm peptide DJK-5 was encapsulated in nanogels composed of octenyl succinic anhydride-modified hyaluronic acid to reduce the toxicity of the peptide. The loaded nanogels were visualized using TEM, while the toxicity and antimicrobial activity was assessed in a murine abscess model. The results show that encapsulation of this peptide in nanogels reduces the peptide's toxicity, maintains antimicrobial activity and provides an immunostimulatory effect.

Table 1.

OSA-HA mg/mL	DJK-5 mg/mL	Size (nm)	PDI	ZP (mV)	EE (%)	Encapsulated (mg/mL)	Supernatant (mg/mL)
10	0	223 ± 7	0.32 ± 0.03	-26.1 ± 0.4	0	0	0
6.6	2	194 ± 3	0.25 ± 0.01	-9.5 ± 0.2	36 ± 4	0.72	1.28
10	3	174 ± 6	0.27 ± 0.05	-9.9 ± 0.5	33 ± 6	0.99	2.01
15	4.5	189 ± 11	0.25 ± 0.03	-11.6 ± 0.3	48 ± 8	2.16	2.34
20	6	179 ± 8	0.30 ± 0.04	-10.2 ± 0.6	35 ± 7	2.10	3.90
25	7.5	176 ± 4	0.24 ± 0.01	-10.5 ± 0.1	60 ± 3	4.50	1.50

Data are presented as mean ± SD (n=3). Abbreviations: OSA-HA: octenyl succinic anhydride-modified hyaluronic acid; PDI: polydispersity index; ZP: zeta potential; EE: encapsulation efficiency.